UDK: 552.52; 621.315.612; 676.017.2, 675.92.027

An Artificial Neural Network-based Prediction Model for Utilization of Coal Ash in Production of Fired Clay Bricks: A review

Milica Vidak Vasić[1*)], Lato Pezo[2], Vivek Gupta[3], Sandeep Chaudhary[3,4], Zagorka Radojević[1]

[1]Institute for Testing of Materials IMS, Bulevar vojvode Mišića 43, 11000 Belgrade, Serbia
[2]University of Belgrade, Institute of General and Physical Chemistry, Studentski trg 12, 11000 Belgrade, Serbia
[3]Discipline of Civil Engineering, Indian Institute of Technology Indore, Simrol, Indore 453552, India
[4]Center for Rural Development and Technology, Indian Institute of Technology Indore, Simrol, Indore 453552, India

Abstract:

This study analyzed the last 20 years` data available on power plant coal ashes used in clay brick production. The statistical analysis has been carried out for a total of 302 cases based on the relevant parameters reported in the literature. The chemical composition of the clays and coal ashes, percentage incorporation and maximum particle size of ash, size of fired samples, peak firing temperature, and the corresponding soaking time were selected as inputs for modeling. The product characteristics i.e. open porosity, water absorption, and compressive strength was taken as output parameters. An artificial neural network model has been developed and showed a satisfactory fit to experimental data and predicted the observed output variables with the overall coefficient of determination (r^2) of 0.972 during the training period. Besides, the reduced chi-square, mean bias error, root mean square error, and mean percentage error were utilized to check the correctness of the obtained model, which proved the network generalization capability. The sensitivity analysis of the model suggested that the quantity of Na_2O coming from brick clays, the percentages of SiO_2 and K_2O coming from ashes, and MgO coming from clays were the most influential parameters in descending order for the ash-clay composite bricks` quality, mostly owing to the influence of fluxes during firing.

Keywords: Clays; Coal ash; Traditional ceramics; Mechanical properties; Modeling.

1. Introduction

Coal ash (CA) is the major waste generated in thermal power plants. Its` quantity is constantly growing with the increase in the number of thermal power plants to meet the huge electricity demand. Coal ashes contain significant concentrations of heavy metals; however, they are not hazardous according to the United States Environmental Protection Agency. The main problems concerning the ashes are their troublesome and costly disposal. They are mostly being used as secondary raw materials in the road embankments, the building construction, and the cement industry [1-3].

_____

*)** Corresponding author:** milica.vasic@institutims.rs

_____

The properties of CAs significantly depend on the quality of coal used and the combustion process. At first sight, the ashes can be broadly divided into two categories: fly ashes (rich in fine particle fraction) and bottom ashes (rich in coarse particle fraction). Fly ash (FA) is gathered from exhaust gases through a dust collector, bag filter, and an electrostatic precipitator. The bottom ash (BA) is gathered from the furnace bottom after incineration. Generally, the thermal power plant generates about 20-80 % of BA, depending on the process conditions and the type of furnace used. BA is considered to be of lower quality since the pozzolanic ability is relatively lower. FA and BA are directly provided to the industries for their effective end-utilization. However, the excess quantities of FA and BA are commonly disposed of in nearby water ponds to minimize the air pollution caused due to fine particles of coal ashes. The mixture of FA and BA found at the disposal ponds is known as pond ash (PA), and is often not a uniform material. The coal ashes differ significantly in physical properties, but may also differ in chemical compositions due to significant variation in unburnt particles [4]. One of the most significant problems for utilization of the ashes arises due to the widely differing quantities of silica and alumina contents [5, 6]. Besides, the quality of CA also depends on the type and the age of coal used and the leftover quantity of calcium after the burning process. For example, the anthracite, as the older deposit, gives the ash containing about 10 wt.% of CaO when burnt, whereas, in the case of the younger sediments (sub-bituminous coal), the coal ash possesses more than 20 wt.% of CaO [5].

The macro-oxides content in coal ashes is somewhat similar to that of brick clays; the main constituents of both materials are silica, aluminum oxide, and iron oxide. This allows the coal ashes to be used in large quantities in the brick industry. In addition to incorporating the waste itself, there are several other environmental advantages concerning the implementation in the brick industry. Coal ash-clay bricks require less energy in the firing phase since most of the ashes` material is already burnt in the thermal power plants. Also, these products are of lower unit weight than traditional ones (up to 10-20 %) which decreases the transport costs, facilitates easier handling, and improve the thermal insulation properties [1]. Intensive research studies were carried out to evaluate the potential of coal ash utilization in the formulations of ash-clay bricks in the last decades [2, 5, 7-17]. Since the chemical composition of the brick clays and coal ashes vary, the present investigation is aimed to summarize all the available results and identify the most influential factors affecting the quality of common clay bricks and coal ash bricks, through a mathematical model. The work explores the suitability of coal ashes in the production of bricks depending on their chemical composition. The database used in the present study consisted of the 302 cases obtained from the available literature for the period from the year 2001 to 2020. In the previous studies [4, 13, 14], Artificial Neural Network was used successfully to predict the mechanical properties of building construction materials. In this study, the parameters of interest concerning the relevant raw materials` and process` parameters were tested using Analysis of Variance, and 25 inputs were chosen to describe 6 outputs (as described in the next section). The Artificial Neural Network (ANN) model was built, and its predictive properties were tested on many levels. The developed model has a practical application by using it as software to predict open porosity, water absorption, and compressive strength of the clay-ash bricks. The model can be updated in the future by including the new data on the same subject, when available. Further, the global sensitivity method was used for determining the influence of the input parameters on the outputs. The important and crucial parameters in defining the final product`s characteristics could be concluded based on this analysis.

2. Materials and Experimental Procedures

The study considered the 302 cases available in the literature on the usage of fly [1, 3-5,7-15,18-30], bottom ashes [2, 6, 24, 30], and pond ashes [5, 13, 14, 31] in clay bricks.

Artificial Neural Networks (ANN) modeling was applied in this study to describe the characteristics of clay bricks (sign b in indexes) and bricks made of coal ash-clay mixtures (sign m in indexes).

2.1. Input and output parameters

The list of inputs included the parameters related to clay and ash characteristics, resultant blended mix, and the other parameters related to the brick manufacturing process as shown in Table I. The parameters related to clay characteristics were the percentage content of major oxides and the loss on ignition of the clay used for brick production. Similarly, the parameters related to ash characteristics were the percentage content of commonly occurring oxides and the loss on ignition of the ash used for brick formulations. The other input parameters were the percentage weight of ash in the resultant blended mix (w/w), maximum particle sizes of the ash (PS_{max}), peak firing temperature (FT), corresponding soaking time at peak firing temperature (StFT), and the bearing surface of samples (S). The output parameters considered were the open porosity (OP_b and OP_m), the water absorption (WA_b and WA_m), and the compressive strength (CS_b and CS_m) for clay bricks and coal ash-clay mixture bricks respectively as shown in Table I.

Tab. I Input and output variables considered in the present study.

Input parameters (25 Nos.)			Output parameters (6 Nos.)	
Clay characteristics (10 Nos.)	Coal ash characteristics (10 Nos.)	Other parameters (05 Nos.)	Clay bricks (3 Nos.)	Coal ash-clay mixture bricks (3 Nos.)
$(SiO_2)_c$	$(SiO_2)_a$	PS_{max}	OP_b	OP_m
$(Al_2O_3)_c$	$(Al_2O_3)_a$	w/w	WA_b	WA_m
$(Fe_2O_3)_c$	$(Fe_2O_3)_a$	S	CS_b	CS_m
$(CaO)_c$	$(CaO)_a$	StFT		
$(MgO)_c$	$(MgO)_a$	FT		
$(Na_2O)_c$	$(Na_2O)_a$			
$(K_2O)_c$	$(K_2O)_a$			
$(TiO_2)_c$	$(TiO_2)_a$			
$(MnO)_c$	$(SO_3)_a$			
$(LOI)_c$	$(LOI)_a$			

The considered input parameters, obtained from the literature, were measured using different methods and techniques. Macro-oxides contents in brick clays and coal ashes were determined by different techniques such as classical silicate analysis [6], X-ray fluorescence spectrometer [1, 3, 9, 11-15, 18, 19, 21, 27, 29, 30], Scanning Electron Microscopy with energy-dispersive X-ray spectroscopy [2], and Inductively Coupled Plasma mass spectroscopy [10]. The results are summarized in Table II.

Particle size distributions of coal ashes were determined by wet [5, 6, 13, 14, 22, 24, 28, 30], and dry sieving [8], while in some studies [1, 3, 9, 11, 12, 25, 29], the samples were sieved or ground and certain fractions were used for the brick production. In the present study, the maximum particle size of the ash (PS_{max}) used for brick production was considered as the input parameter.

The samples were cast by hand in a mold [25, 26, 31], hydraulically pressed [2, 3, 5, 8, 11, 18, 22, 29, 30], or shaped in a vacuum extruder [1, 9, 10, 13-15, 19, 21, 27, 30]. In most of the studies considered, dimensions of the samples were determined by caliper, and the sample's bearing surface was calculated. In the present study, the bearing surface of the specimen (S) was considered as representative of size in the list of input parameters.

Tab. II Chemical composition of the brick clays and the coal ashes.

Brick clays	$(Al_2O_3)_c$ (%)	$(SiO_2)_c$ (%)	$(Fe_2O_3)_c$ (%)	$(CaO)_c$ (%)	$(MgO)_c$ (%)	$(Na_2O)_c$ (%)	$(K_2O)_c$ (%)	$(TiO_2)_c$ (%)	$(MnO)_c$ (%)	LOI_c (%)
Min	5.80	46.88	2.66	0.27	0.06	0.00	0.45	0.00	0.00	0.00
Max	21.89	81.10	16.32	10.30	8.15	2.36	8.27	1.90	0.47	5.57
Average	13.87	58.62	6.39	5.20	2.25	1.22	2.39	0.77	0.07	0.65
Standard deviation	3.16	8.56	3.02	2.92	1.95	0.74	1.29	0.73	0.12	1.49
Coal ashes	$(Al_2O_3)_a$ (%)	$(SiO_2)_a$ (%)	$(Fe_2O_3)_a$ (%)	$(CaO)_a$ (%)	$(MgO)_a$ (%)	$(Na_2O)_a$ (%)	$(K_2O)_a$ (%)	$(TiO_2)_a$ (%)	$(MnO)_a$ (%)	LOI_a (%)
Min	7.14	16.17	2.41	0.59	0.00	0.00	0.00	0.00	0.00	0.00
Max	63.67	67.40	16.52	26.02	4.94	13.45	5.19	2.80	1.29	10.34
Average	18.86	44.26	7.27	10.07	1.81	1.90	1.77	0.72	0.11	3.00
Standard deviation	9.53	16.69	3.56	9.49	1.23	2.73	0.88	0.73	0.28	3.99

Index c refers to the brick clays, and the index a refers to the ashes.

The firing was done in an electric furnace [2, 3, 5, 6, 8, 11-14, 18-23, 29, 30], tunnel kiln [1, 9, 10, 27], or in a primitive chamber kiln [1, 15, 25, 26, 28, 31] , in the temperatures range 750-1300 °C. In the present study, the peak firing temperature (FT), and the corresponding soaking time at peak firing temperature (StFT) were considered as representative of the manufacturing process in the list of input parameters.

Similarly, the considered output parameters were measured using different methods and techniques. The open porosity (OP_b and OP_m) of bricks was calculated after measuring the weight of dry samples, and saturated wet samples in the air and water according to the standard procedure [1, 2, 3-5, 12-14, 20, 29, 30]. The water absorption (WA_b and WA_m) of bricks was determined in a standard way using the water-saturated weight and the oven-dried weight. The samples were soaked in distilled water in ambient conditions, whereas, in some studies [1-3, 5, 9, 11, 12-15, 21, 23-31], the water absorption was determined by the boiling method. The bricks were tested for compressive strength (CS_b and CS_m) using a hydraulic press and by following the standard procedure [1-5, 9, 10-15, 18, 20, 22-26, 28-31].

2.2. Statistical analysis and Artificial Neural Network modeling

The STATISTICA 10.0 (StatSoft Inc. Tulsa, OK, USA) software was used for testing the data and the ANN modeling. The gathered database of the considered 302 cases is first examined using Principal Components Analysis to test the variability of the parameters, and then, the input and output parameters (as previously shown in Table I) were selected for ANN modeling. Artificial Neural Networks were built following the procedure which was the most efficient as per the previous studies on a similar subject [13, 14, 32-35]. A multilayer perceptron model consisting of three layers was used for building the network, while constantly minimizing the differences between the network predicted and experimental results. Thus, Broyden– Fletcher–Goldfarb–Shanno (BFGS) algorithm is utilized within the program. The coefficient of determination (r^2), reduced chi-square (χ^2), mean bias error, and also root mean square and mean percentage errors were used to check the correctness of the obtained model [34, 36].

2.3. Global sensitivity analysis

This study consisted of 25 input variables, which would make the classical sensitivity analysis very complex [37], so the influence of the input parameters on the output parameters (properties of final brick products) was simultaneously analyzed using the global sensitivity method for establishing the relative importance of each variable on the model output [38]. The relative importance of the input variables is estimated using Equation 1, according to the methodology previously proposed for global sensitivity analysis [39]:

$$RI_{ij}[\%] = \frac{\sum_{k=0}^{n}(w_{ik}w_{kj})}{\sum_{i=0}^{m} abs \sum_{k=0}^{n}(w_{ik}w_{kj})} \; 100 \; \% \qquad (1)$$

where RI_{ij} presents the relative importance of the ith input variable on the jth output, w_{ik} means the weight between the ith input and the kth hidden neuron, and w_{kj} is the weight between the kth hidden neuron and the jth output, while *abs* represent the absolute value.

3. Results and Discussion
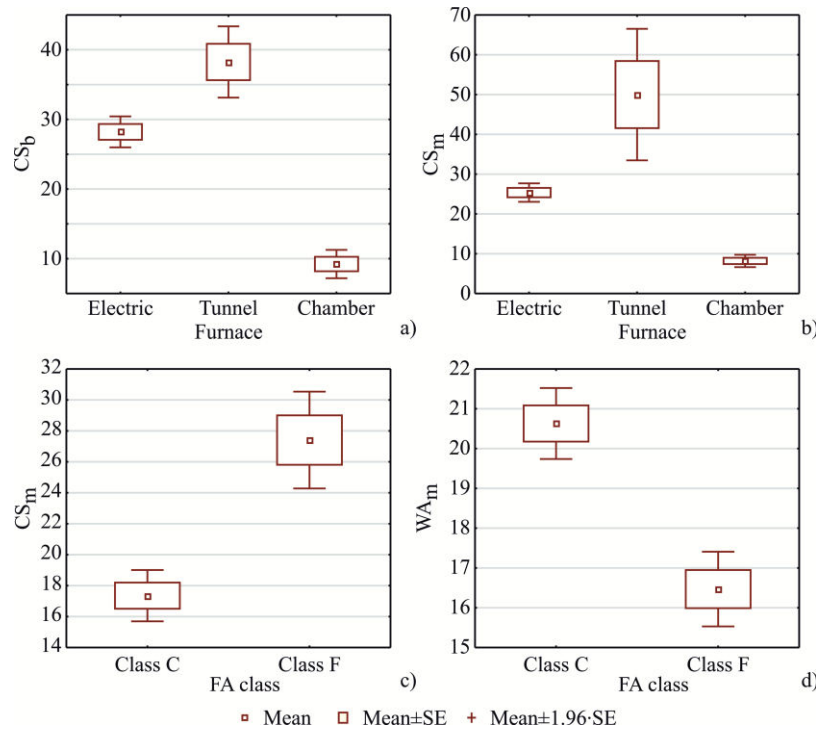
Fig. 1. ANOVA analysis of the 20 years literature database using selected categorical parameters: (a) compressive strength of clay bricks (CS_b) concerning the used furnaces, (b) compressive strength of coal ash-clay bricks (CS_m) dependence on the used furnaces. (c) dependence of compressive strength of coal ash-clay bricks (CS_m) on the type of the ashes, and (d) water absorption of coal ash-clay bricks (WA_m) related to the coal ashes class.

The first-hand analysis of the database was done by observing the percentual differences of clay bricks and coal ash-clay bricks characteristics (open porosities, water absorptions, and compressive strengths). The highest average changes in coal ash-clay bricks were observed in water absorption values (+17.44 %), while changes in open porosities were a bit lower (+12.57 %). The compressive strengths were lowered with the addition of coal ashes for 4.63 % on average. The general rule is that the unburned parts of the ashes introduced the new pores in the system while decreasing the strength of the fired products [8, 28, 30]. In some of the studies, the changes in product quality were vice-versa (improved compressive strength or/and lowered water absorption in coal ash-clay bricks compared to clay bricks) [2, 6, 26, 40]. Besides, with the addition of coal ashes up to 60 %, WA_m was up to about 20 %, and with a higher share of coal ashes, it went up to over 40 %. Generally, the amounts of waste higher than 50 % introduced more significant changes to the outputs. However, the higher contents of CA in the mixtures are not a constraint in the quality of products [14]. It must be emphasized that the increased content of the ashes lowers the plasticity and makes the

_____

extrusion process difficult if the plasticizer is not added [2]. In the case of maximally increased values of CS_m and OP_m, it seems that the reason behind is not the content of the ash, but the chemical composition (mostly the quantity of CaO, MgO, Al_2O_3, and SiO_2). WA maximally decreased in the cases when there was more or equal to 65 % of SiO_2 and up to about 6 % of CaO and MgO in the clay-ash mix [1, 9, 18, 25]. These general remarks were further checked and analyzed in-depth with the use of mathematical modeling and analysis.

  The literature-gathered database was at first checked using Analysis of Variance to test the variability of the input parameters. The parameters that showed low variability were the contents of SO_3 in brick clays (0.65 % on average) and the contents of MnO in the ashes (0.11 % on average), and thus they were excluded from the modeling. Box & Whisker plots for the output parameters are shown in Fig. 1. The performance of the bricks fired in different furnaces is compared in Fig. 1a and Fig. 1b. The compressive strengths were found to be the highest for the samples fired in tunnel kilns as compared to products fired in electric furnaces and chamber kilns for both clay bricks and coal ash-clay bricks. When the coal ash with a higher CaO content (the ash of class C) was used, the values of WA_m were found higher than the cases using class F ashes. The compressive strength, CS_m was also lower in the case of the ash of class C (Fig. 1). This indicated that class F ashes are more favorable to be used in the brick industry, which is already observed earlier [21].

  Principal components analysis is done to present the positions of the samples and output parameters in an orthogonal space. The used methodology was in more details explained in the previous study [14]. Based on the statistical analysis of the observed outputs, it is seen that there were two statistically significant factor coordinates. In factor 1, the variances that participated the most were of OP_c, OP_m, WA_c, and WA_m. The factor 2 constituted mostly of CS_c and CS_m. Eigenvalues of these two factors contributed to a high ability to describe the chosen parameters since they covered about 84 % of the system variability. It is evident from Fig. 2 that water absorption and open porosity of pure clay bricks and the mixed ash-clay bricks were positively correlated, while the increase in OP, Opm, WA, and Wam meant the decrease in CS and CSm.
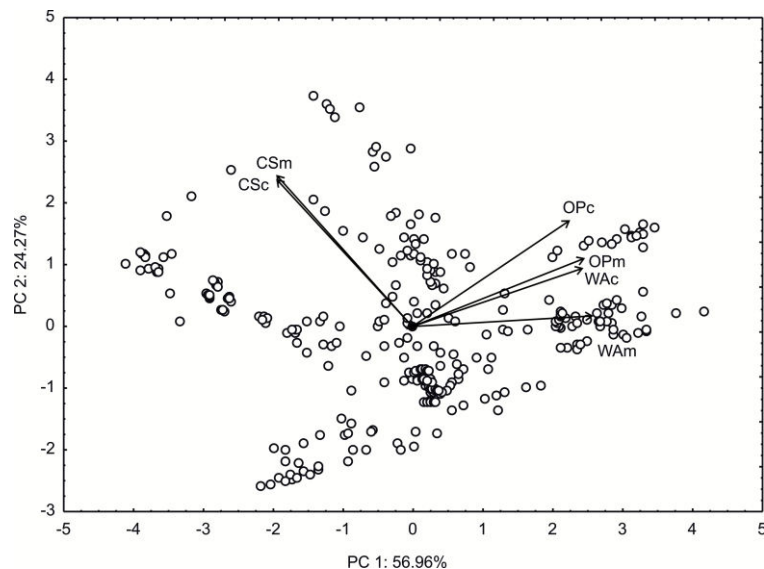

Fig. 2. Principal components analysis of the characteristics of the fired samples.

  To sum the effects of the observed inputs over the outputs, the contour plots were made and shown in Fig. 3 and Fig. 4. The weight percent of the added ashes considerably increased water absorption and decreased compressive strength, but the firing temperature is

_____

more influential then w/w (Fig. 3b). CSm increased with the rise of FT and StFT, as seen in Fig. 3c. The researchers used peak temperatures between 1140 and 1300 °C in the case of higher w/w (in between 60 and 90 %) when WAm was up to 10 % (Fig. 3d). Considering the chemical content, more calcite in clay and lower amounts of K_2O in the ashes increased the water absorption (Fig. 4a), the complicated relationships of silica and K_2O from the ashes and $(Na_2O)_c$ are seen in Fig. 4b, Fig. 4c, and Fig. 4d. It is concluded that the relationships between the followed parameters are very complex and that mathematical modeling must be employed.
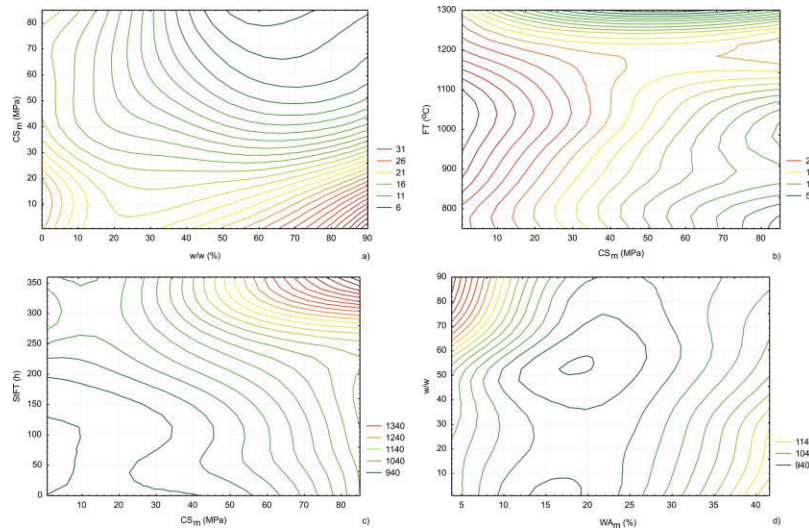
Fig. 3. The technological and processing parameters` relationships: (a) WA_m against CS_m and w/w, (b) WA_m against FT and CS_m, (c) FT against CSm and StFT, and (d) FT against WAm and w/w.
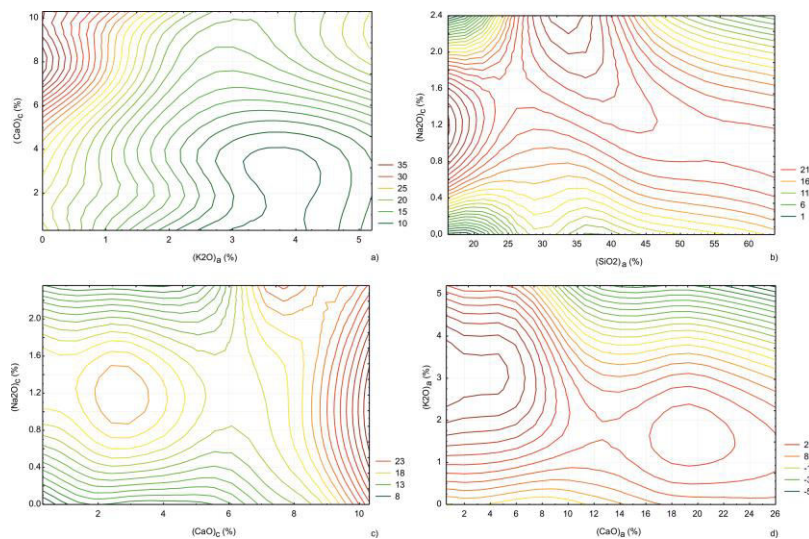
Fig. 4. The influence of chemical content of the raw materials to the final properties of clay-ash bricks: (a) WA_m against $(CaO)_c$ and $(K_2O)_a$, (b) WA_m against $(Na_2O)_c$ and $(SiO_2)_a$, (c) WA_m against $(Na_2O)_c$ and $(CaO)_c$, and (d) CS_m against $(K_2O)_a$ and $(CaO)_a$ (%).

_____

3.1. ANN modeling

Artificial Neural Networks (ANN) modeling was applied in this study to describe the characteristics of common clay bricks and bricks made of coal ash-clay mixtures. Since there was no sufficient data in the literature regarding firing in a tunnel and chamber furnaces, the variable that could distinguish the type of the furnace used was not considered as an input parameter. However, it is indirectly contained in the parameter describing the soaking time at peak temperature. A similar situation was with the categorical parameter that would describe the type of coal ashes. However, that information was again included indirectly in the chemical analysis. It must be emphasized that introducing the parameter that is already contained in the inputs lowers the quality of the developed network.

According to the ANN performance, the optimal number of neurons in the hidden layer for the six output parameters (OP_b, OP_m, WA_b, WA_m, CS_b, and CS_m) was 17 (network MLP 25-17-6). The network gave high values of r^2 (overall 0.972, during the training period) and low values of SOS (Table III). The goodness of fit between experimental measurements and model calculated outputs, represented as ANN performance (sum of r^2 between measured and calculated output parameters OP_b, OP_m, WA_b, WA_m, CS_b, and CS_m), during training, testing, and validation steps, are shown in Table IV. Samples for these steps were chosen using the random function, by dividing the collected database to 60 % for training, and 20 % each for testing and validation [37].

Tab. III Summary of the parameters related to the developed ANN model.

Network name	Network performance			Network error			Used algorithms and functions			
	Train-ing	Test	Validat-ion	Training	Test	Validatio-n	Traini-ng algorit-hm	Error functi-on	Hidden activation	Output activation
MLP 25-17-6	0.972	0.891	0.919	13.447	61.890	59.101	BFGS 129	SOS	Exponent-ial	Logistic

Tab. IV Coefficients of determination (r^2) between experimentally measured and ANN outputs during training, testing, and validation steps.

|	OP_b	OP_m	WA_b	WA_m	CS_b	CS_m
Training	0.991	0.960	0.991	0.951	0.977	0.964
Testing	0.953	0.776	0.952	0.883	0.889	0.899
Validation	0.989	0.884	0.996	0.871	0.941	0.839

ANN models predicted the output values (OP_b, OP_m, WA_b, WA_m, CS_b, and CS_m) satisfactorily for a broad range of the chosen parameters. This conclusion can be seen in Fig. 5, where the experimentally measured and the ANN model's predicted values of the outputs are presented as r^2 values. The least scattering of the results was observed with the standard bricks. CS_m showed the lowest accuracy during prediction, which means that the high variability of the results is obtained, which may be caused by the different dimensions of the samples.

ANN models were highly complex (720 weights-biases) because of the intensive nonlinearity of the developed system [37]. The values of r^2 between experimental and ANN model outputs were between 0.951-0.991 during the training period (Table IV).

The quality of the model fit and the residual analysis were tested and presented in Table V. The ANN model showed a minor lack of fit tests, which means the model satisfactorily predicted the ANN outputs. To test the accuracy of the models, several methodologies were used (the coefficient of determination, r^2; the sum of squares, SOS; reduced chi-square, χ^2; mean bias error, MBE; root mean square error, RMSE; and mean

percentage error, MPE) [37]. The predicted values were very close to the desired values (Table IV and Fig. 5). Error functions (SOS) obtained with the ANN models were of the same order of magnitude as in experimental errors.
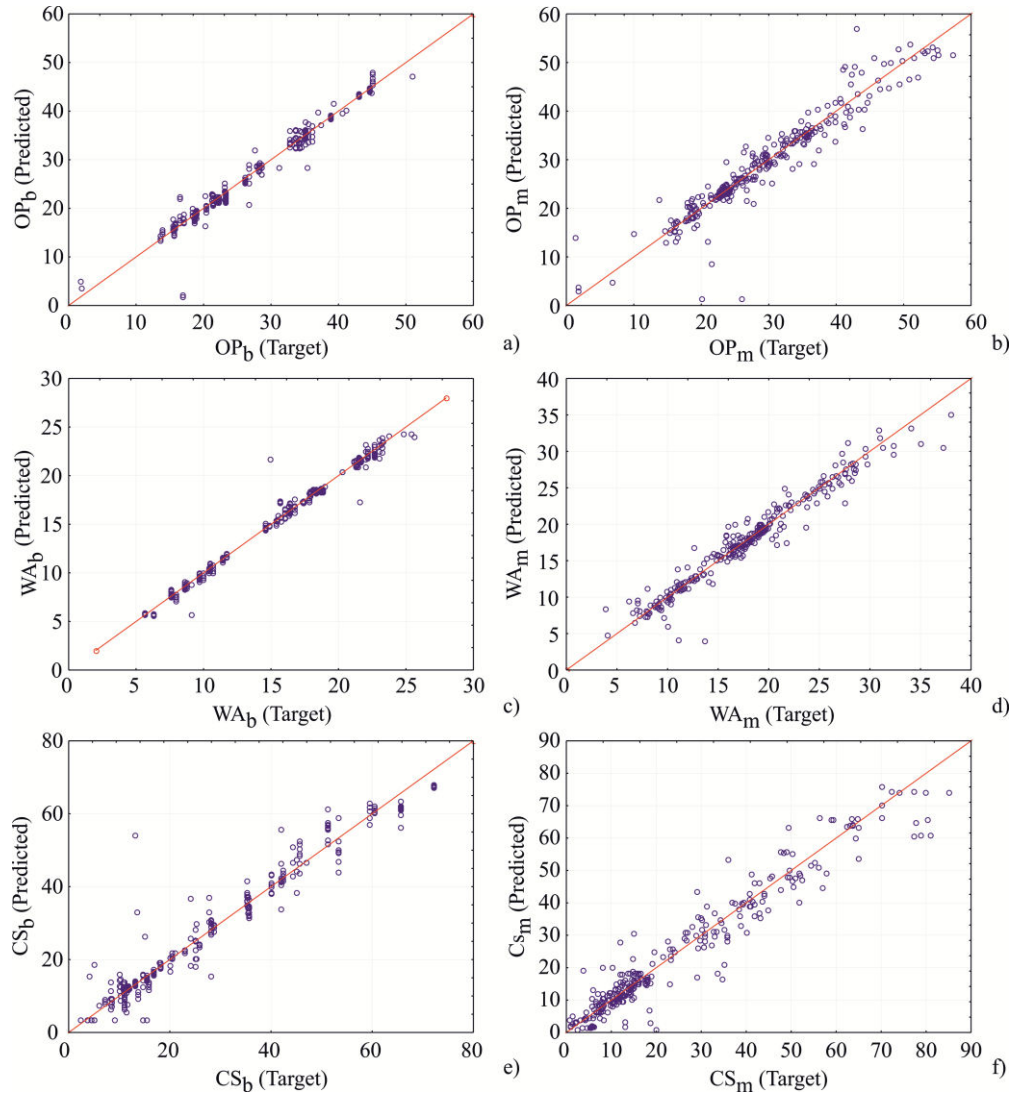
Fig. 5. Experimental and predicted values obtained for (a) open porosity of clay bricks, (b) open porosity of coal ash-clay bricks, (c) water absorption of clay bricks, (d) water absorption of coal ash-clay bricks, (e) compressive strength of clay bricks, and (f) compressive strength coal ash-clay bricks.

Tab. V Calculated parameters for the applied artificial neural networks.

Output	Reduced chi-square	Root mean square error	Mean bias error	Mean percentage error
OP_b	3.451	1.837	-0.050	5.261
OP_m	11.512	3.355	0.008	11.279
WA_b	0.513	0.708	0.039	2.780
WA_m	2.840	1.666	0.027	6.712
CS_b	20.745	4.504	-0.207	15.525
CS_m	30.676	5.477	0.411	26.445

_____

3.1.1. The matrix for prediction of the quality of bricks

The computation of the outputs using the obtained ANN model is presented in the following Equation:

$$Y = f_1(W_2 \times f_2(W_1 \times X + B_1) + B_2) \qquad (2)$$

where W_1 and B_1 represent the matrices associated with the hidden layer (weights and biases), while the output layer is presented with W_2 and B_2. Y is the matrix of the output variables, f_1 and f_2 are transfer functions in the hidden and output layers, respectively, X is the matrix of the input variables. An exponential function was used in the hidden layer, while the logistic function is used as a transfer function in the output layer.

Output variables can be calculated by applying transfer functions f_1 and f_2 in the hidden and output layers, respectively, onto the matrix of input variables X using Eq. (1). Table VIa-b presents the elements of matrix W_1 and vector B_1 (presented in "bias" column), while Table VIIa-b presents the elements of matrix W_2 and vector B_2 ("bias" raw) for the hidden layer.

Tab. VIa Elements of matrix W1 and vector B1 (presented in the "bias" column).

Hidden neuron Input parameter	1	2	3	4	5	6	7	8
$(Al_2O_3)_c$	0.263	1.347	0.240	-1.254	-0.112	0.662	1.370	-0.472
$(SiO_2)_c$	-0.411	0.214	-0.125	-0.307	0.607	-0.250	-0.674	0.827
$(Fe_2O_3)_c$	-0.340	-0.543	-0.215	-0.161	-0.940	-1.333	-0.240	1.555
$(CaO)_c$	-0.230	-2.562	-0.297	-1.326	-0.021	-0.348	-2.708	-1.334
$(MgO)_c$	0.602	0.774	0.786	-1.080	0.723	2.710	1.945	0.761
$(Na_2O)_c$	-1.234	1.402	-1.104	-1.373	-1.197	-1.205	0.375	0.026
$(K_2O)_c$	-0.235	0.437	-0.253	-0.364	0.024	-0.273	-2.910	0.232
$(TiO_2)_c$	-0.924	2.782	-0.944	-0.135	-0.996	0.470	-0.875	-1.144
$(MnO)_c$	-0.341	-1.835	-1.604	-0.008	-2.346	0.066	-0.672	-0.403
$(LOI)_c$	-0.078	-2.108	-0.883	0.439	-0.203	-0.571	-1.053	-0.175
$(Al_2O_3)_a$	0.295	0.422	-0.324	0.264	0.025	0.960	0.696	-1.923
$(SiO_2)_a$	0.409	-2.148	0.247	0.971	-1.825	-1.320	1.142	-0.968
$(Fe_2O_3)_a$	0.269	-1.520	-1.031	-0.102	-2.030	-1.311	0.285	0.155
$(CaO)_a$	0.203	1.746	-0.284	-0.227	1.597	1.372	1.746	0.982
$(MgO)_a$	0.250	-0.305	0.515	-0.475	0.421	0.955	0.498	0.181
$(Na_2O)_a$	-0.946	-1.206	-0.596	-0.336	-0.911	-1.888	0.281	0.299
$(K_2O)_a$	-0.578	-0.679	-0.265	0.383	-0.288	-0.335	-0.267	0.415
$(TiO_2)_a$	-1.258	-0.250	-1.411	-0.677	-1.120	0.908	0.363	-1.657
$(SO_3)_a$	0.067	0.701	0.969	0.630	-0.669	-0.490	-1.922	-0.012
$(LOI)_a$	-0.051	-0.378	1.246	1.489	-1.529	-0.928	-1.541	-0.613
w/w	0.370	-0.141	0.628	0.218	0.383	1.349	0.272	-0.217

_____

PS_{max}	-0.891	0.212	-1.977	1.810	-1.024	-1.623	0.845	-0.379
StFT	0.444	0.455	1.235	0.289	1.193	-0.971	2.151	0.008
FT	-0.446	-1.081	-0.521	1.077	1.911	1.222	0.499	-0.126
S	0.902	2.308	3.010	0.579	1.727	0.313	0.000	0.266
Bias	-0.270	-0.286	-0.478	-0.839	0.066	-0.180	-0.580	0.730

Tab. VIb Elements of matrix W1 and vector B1 (presented in the "bias" column).

Hidden neuron / Input parameter	9	10	11	12	13	14	15	16	17
$(Al_2O_3)_c$	-1.053	-0.584	-1.346	-0.186	-0.629	-1.143	-0.151	-1.092	0.254
$(SiO_2)_c$	1.473	0.568	-0.548	-0.221	0.270	0.844	-0.952	1.461	1.231
$(Fe_2O_3)_c$	-1.509	0.140	-0.373	-0.167	-0.496	-0.775	-0.906	-0.446	0.860
$(CaO)_c$	-0.387	-1.154	-0.854	-0.612	0.758	-0.831	-0.495	-0.322	1.136
$(MgO)_c$	0.985	-0.075	0.771	1.843	1.287	-0.214	1.071	-2.000	0.497
$(Na_2O)_c$	0.182	0.501	0.237	-0.911	-0.253	-1.254	-0.354	2.668	-0.866
$(K_2O)_c$	0.293	0.524	0.426	0.320	-0.435	0.230	-2.071	0.498	-0.597
$(TiO_2)_c$	-0.904	0.916	-1.122	-0.442	3.625	-0.836	0.709	0.383	-1.249
$(MnO)_c$	-0.312	-1.649	-0.946	-0.857	0.302	-2.018	-0.500	-2.531	-0.224
$(LOI)_c$	-1.057	0.403	-0.767	-0.242	1.210	-0.404	0.946	-0.619	-1.175
$(Al_2O_3)_a$	0.351	0.200	0.069	0.583	1.607	0.262	3.081	0.555	-0.776
$(SiO_2)_a$	2.353	-0.959	-0.447	0.152	-0.921	-0.867	-0.652	-0.689	-1.487
$(Fe_2O_3)_a$	-1.783	-1.076	-0.494	-0.546	0.507	-1.212	-1.546	-1.122	-2.469
$(CaO)_a$	-0.948	-0.030	1.837	1.776	-1.872	0.545	1.002	0.099	-1.118
$(MgO)_a$	-0.961	0.628	-0.281	0.195	-0.688	-0.454	0.233	-0.957	1.575
$(Na_2O)_a$	-0.853	-0.123	-1.185	-1.335	-0.194	-1.387	-1.216	-0.245	0.416
$(K_2O)_a$	-4.542	-1.026	-0.816	-1.721	-0.238	-1.154	2.197	-1.058	-1.243
$(TiO_2)_a$	-0.693	-0.203	-1.394	0.215	-1.672	-0.741	-0.279	-2.398	0.354
$(SO_3)_a$	0.330	-2.191	-0.453	0.356	0.714	0.074	0.102	-0.706	-1.267
$(LOI)_a$	3.810	-3.506	0.448	-0.227	-0.304	1.117	-1.908	-0.377	0.839
w/w	0.882	0.227	1.082	-1.768	-0.092	0.302	0.424	0.445	1.117
PS_{max}	0.056	-0.936	-1.597	-0.780	-1.785	-1.205	-2.642	-1.233	0.773
StFT	-0.899	1.979	0.767	0.115	0.231	2.692	1.407	0.102	0.534
FT	1.301	-0.519	3.033	0.337	-1.779	-0.028	0.986	2.975	1.010
S	1.765	0.634	0.751	1.319	-0.425	2.480	-2.645	1.541	1.127
Bias	0.166	0.367	-1.316	-0.673	0.379	-0.477	-0.676	-0.140	0.524

Tab. VIIa Elements of matrix W2 and vector B2 ("bias" raw).

Hidden neuron / Output parameter	1	2	3	4	5	6	7	8	9	10
OP_c	0.659	0.367	-0.172	-0.502	-1.566	0.078	-0.819	-0.704	0.229	-0.269
OP_m	-0.102	0.417	-0.206	1.066	-0.968	0.231	-0.557	-0.002	0.861	0.512
WA_c	-1.107	0.436	-0.921	-2.538	1.424	0.088	-1.622	-0.136	0.373	1.102
WA_m	-1.122	0.340	-0.325	0.379	1.519	0.451	-1.095	0.747	0.873	1.970
CS_c	-0.811	-2.316	1.098	0.274	0.819	0.727	-1.650	-3.067	-1.063	0.177

_____

CS_m	0.224	-0.817	1.066	-1.440	0.376	0.226	-1.185	-2.965	-1.364	-0.781
Bias	0.659	0.367	-0.172	-0.502	-1.566	0.078	-0.819	-0.704	0.229	-0.269

Tab. VIIb Elements of matrix W2 and vector B2 ("bias" raw).

Hidden neuron / Output parameter	11	12	13	14	15	16	17	Bais
OP_c	0.816	0.381	0.042	0.948	0.620	-0.154	-0.362	0.511
OP_m	1.093	-0.462	0.162	0.801	1.084	-1.441	-1.096	-0.639
WA_c	-0.721	-0.118	0.126	1.286	0.204	-0.469	0.268	1.215
WA_m	-0.358	-1.627	0.122	0.196	0.701	-1.687	-0.694	-0.709
CS_c	0.240	-0.365	-1.224	0.720	-0.918	1.770	-1.399	5.083
CS_m	1.033	0.371	-0.951	-0.113	-1.235	2.673	-1.281	4.247
Bias	0.816	0.381	0.042	0.948	0.620	-0.154	-0.362	0.511

3.2. Global sensitivity analysis - the relative importance of parameters

The method of weights partitioning [39] allows for determining the relative importance of the input parameters over the output parameters of ANN. The weights between the input, hidden, and output layers are used to calculate the relative importance of each of the input parameters (Fig. 6).

The highest influence on a global model behavior is determined in the case of concentration of fluxes in the mixtures. The highest relative importance was found in the case of concentration of Na_2O in brick clays, then the quantity of SiO_2 and K_2O in the coal ashes, and at last the concentration of calcite and magnesite in the clays. Na_2O in clays is found mainly in the form of feldspar albite ($NaAlSi_3O_8$), which is made up of particles larger than 10 μm. Since plasticity increases with the increase in finer particle fraction (below 2 μm), the coarser fraction not only lowers the plasticity, susceptibility to drying, and drying shrinkage, but also the water absorption and the open porosity. Free Na_2O is also an important flux in these systems, that lower the melting point of the matrix. Besides, the remaining amorphous phase in the fired products also depends on the content of feldspars [41].
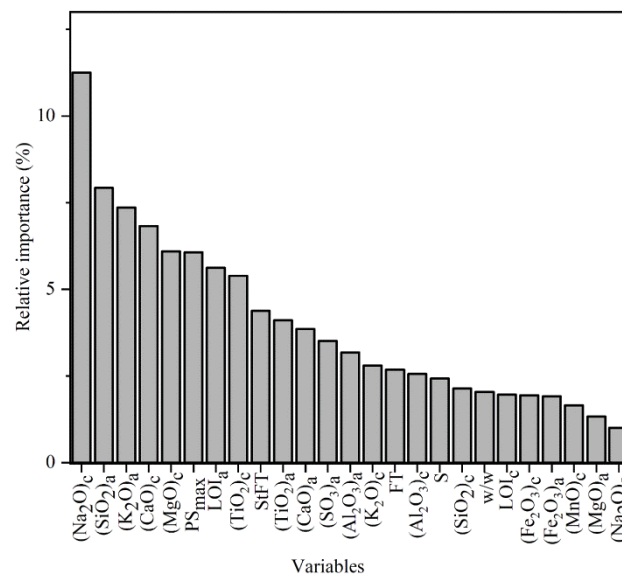
Fig. 6. The relative importance of the ANN input parameters.

_____

The importance of SiO_2 is ascertained by the fact that the ashes contain silica partly as quartz and partly in the form of other compounds such as mullite, anorthite, or cristobalite. Since silica was found in higher concentrations in clays than the ashes, the higher contents of the ashes decreased the overall percentage content of silica in the mixtures, and especially quartz [2], which increased water absorption and decreased compressive strength of the products. Quartz in ceramic bodies is important as its higher quantity can lower the matrix strength and decrease the melting point [36, 41]. The quantity of large-sized particles, which lowers the strength during the cooling phase and increases the open porosity, is decreased with the addition of the ashes [36]. The addition of coal ashes lowered the contents of SiO_2, K_2O, CaO, and MgO in the matrix, which means that the fluxing characteristics are weaker when compared to the primary clay material [36, 43]. Also, calcium-oxide can react with quartz or alumina/silica from clay minerals during high- temperature decomposition and form silicates, which increase compressive strength. In here present cases, it seems that this reaction rarely occurred since the clays were not rich in clay minerals or the carbonate grains were large. Grains of CaO larger than 1 mm increase porosity. The decreased content of $(CaO)_c$ influenced the drop in WA of the ash-clay bricks, as shown in Fig. 4.

The next in the line by the importance is the maximum particle size of the ashes. It is known that brick quality depends on the particle size of the raw materials as smaller particles enable faster sintering while forming more of a glassy phase, improving compressive strength, and eliminating the pores. Fine particles of CA reduce the final firing temperature, while the coarse particles promote crystallization, increase porosity, and lower the strength of the products [29].

LOI of CAs was higher than that of brick clays on average. Its importance is reflected in the fact that the ashes contain the remaining combustible components that give additional energy to the system. It is known that this parameter defers the low (high LOI results) and high (low LOI values) grade fly ash. Besides, the newly-introduced pores improve the insulating properties of the final bricks. The increased LOI generally influenced higher WA_m values, but this parameter also showed a combined effect with the other, such as the origin of the burnt matter (carbonates or organic compounds).

TiO_2 in clays is considered as somewhat impassive. Titanium can be present in the form of oxide or titanate, as a constituent of hematite or rutile. Rutile is one of the most widely recognized minerals of titanium which appears as a supporting mineral in mica, granite, limestone, dolomite, quartz, hematite, and feldspar, which explains its` importance.

The soaking time at the final temperature was found to be the important input parameter [41]. It contained the information on the type of furnace used since industrial conditions require long soaking times. In the references included in this study, the soaking times in electrical furnaces varied from 0–10 h. There was only one variant for the soaking time (40 h) in the tunnel kiln, while in the chamber kilns the times varied from 72–360 h.

TiO_2 introduced with the ashes showed an opposite influence compared to that of clays, since its` increased contents decreased open porosity and water absorption.

CaO was present in the ashes in higher quantities than that in brick clays, and it greatly affected the compressive strength of the products by lowering it. The calcite in clays was probably present in finer particle sizes, while in the ashes the grains were coarser. As mentioned before, the high CA quantities (above 50 %) significantly lower the quality of bricks in terms of compressive strength [45].

Class F ashes contain low SO_3 concentrations [46], but the higher contents are seen in ashes of Class C. The impact of sulfates from CAs was much more important than that of brick clays. The average content of SO_3 in CAs was 3.46 %, while clays contained 0.68 %. With the higher addition of CAs, in the reduction atmosphere, there is a possibility of calcium sulfide occurrence. A black reduction core in the product lowers the compressive strength and the frost resistance [47].

_____

The importance of the composition of Al_2O_3 in the ashes reflected probably in the presence of mullite, which slightly lowered compressive strength and intensively increased water absorption [48].

Firing temperature, the surface of the samples, and the quantity of the added ashes were not as significant parameters as the others. It seems that the chemical composition of the two raw materials plays the greatest role in the final product quality.

This study can be improved, when more valuable data is available. The more numerous data concerning the firing of coal ash clay bricks in tunnel and chamber kilns are needed. Also, there is a lack of research studies related to bottom and pond ash usage in clay brick production. Besides the usually followed parameters that characterize the final brick products, more information is needed regarding their durability and frost resistance [48].

4. Conclusion

The leading idea of this study was to systematically analyze the usage of coal ashes generated in thermal power plants in clay bricks production. The database consisted of 302 cases incorporating 1 wt.% - 90 wt.% of different types of coal ashes (fly, bottom, and pond ashes). The raw materials (clays and ashes) were characterized by the major oxides contents. Besides, the other ashes` characteristics i.e. particle size and quantity of ash incorporated were considered for modeling. The manufacturing parameters such as the size of the fired products, firing temperature, and the corresponding soaking time were also accounted for in the model. The product`s quality was described by open porosity, water absorption, and compressive strength for both the common clay bricks and the ash-clay bricks. The mathematical model is developed using Artificial Neural Networks which, by their high values of coefficients of determination and satisfactory fitting to the experimental data, can be used as software for predicting the quality of the products based on the raw material characteristics, composition, and processing conditions. Taking into account that a considerable amount and wide variety of data had been used to obtain the ANN models, it is expected to be very useful as a simple way to preliminary decide the product characteristics. The simulated values obtained from the ANN model were close to the actual values, thus the ANN model can act as a decision support system to attain the desired objective in the production of coal ash-clay bricks.

A global sensitivity analysis of the obtained models followed, which highlighted the greatest impacts of the studied parameters. It was found that the composition of the fluxes (Na_2O, CaO, and MgO originating from the clay, and K_2O introduced with the ashes) played the most important role in the quality of final products. Besides, silica introduced with the coal ashes showed up to be influential since lowering its total content in the matrix and thus demoting the appearance of silicates during firing.

Most of the literature is focused on the viability of making bricks from mixtures of clay and coal combustion residues with emphasis on the resulting physical and mechanical properties, but further investigations on the durability of products are needed. Besides, more experiments on firing coal ash clay bricks in tunnel and chamber kilns would be valuable in enriching the database, which would improve the model and consequent conclusions.

Acknowledgments

_____

5. References

1. M. M Chou, V. Patel, C. J. Laird, K. K. Ho, Energ. Source., 23(7) (2010) 665-673.
2. B. Sena da Fonseca, C. Galhano, D. Seixas, Appl. Clay Sci., 104 (2015) 189-195.
3. H. Singh, G. S. Brar, G. S. Mudahar, J. Build. Phys., 40(6) (2017) 530-543.
4. V. Gupta, D. K. Pathak, S. Siddique, R. Kumar, S. Chaudhary, Constr. Build. Mater., 235 (2020) 117413.
5. R. Sarkar, N. Singh, S.K. Das, Waste Manage. Res., 25 (2007) 566-571.
6. A. Bilgil, M. Uçurum, M. V. Gökçe, M. Fener, E. Yeşilyurt, OHU J. Eng. Sci., 6(2) (2017) 483-491, ISSN: 2564-6605
7. R. Güler, P. Patla, T. R. Hess, R. K. Vempati, D. L. Cocke, J. Environ. Sci. Health, A30(3) (1995) 505-524.
8. T. Fatih, A. Ümit, Utilization of fly ash in manufacturing of building bricks, International Ash Symposium, Center for Applied Energy Research, University of Kentucky, 2001.
9. M. M Chou, F. Botha, Manufacturing commercial bricks with Illinois coal fly ash – A program overview, International Ash Utilization Symposium. Center for Applied Energy Research, University of Kentucky, 2003, Paper 25.
10. F. Andreola, L. Barbieri, I. Lancellotti, P. Pozzi, Mater. Construcc., 55(280) (2005) 5-16.
11. K. Koseoglu, M. Polat, H. Polat, J. Haz. Mater., 176 (2010) 957-964.
12. M. S. Sultana, M. I. Hossain, M. A. Rahman, M. H. Khan, J. Sci. Res., 6[3] (2014) 421-430.
13. M. Arsenović, Z. Radojević, Ž. Jakšić, L. Pezo, Ceram. Int., 41(3) (2015) 4890-4898.
14. M. Arsenović, Z. Radojević, Ž. Jakšić, L. Pezo, Ceram. Int., 41(3) (2015) 4899-4905.
15. K. Srinavin, P. Tunming, Key Eng. Mater., 718 (2016) 169-176.
16. A. K. Mandal, O. P. Sinha, J. Mater. Civ. Eng. 29(4) (2017) 04016245.
17. K. Gourav, B.V.V. Reddy, J. Mater. Civ. Eng., 30(9) (2018) 04018202.
18. X. Lingling, G. Wei, W. Tao, Y. Nanru, Constr. Build. Mat., 19 (2005) 243-247. https://doi.org/10.1016/j.conbuildmat.2004.05.017
19. X. Spiliotis, V. Karayannis, N. Koukouzas, D. Kasidakis, D. Papanikolaou, A. Riga, G. Papapolymerou, Physico-mechanical properties of clay bricks containing recycled lignite fly ash, 10th International Conference and Exhibition of the European Ceramic Society, Berlin, Germany, June 17-21, 2007.
20. G. Cultrone, E. Sebastián, Constr. Build. Mat., 23 (2009) 1178-1184.
21. N. Koukouzas, C. Ketikidis, G. Itskos, X. Spiliotis, V. Karayannis, G. Papapolymerou, Waste Biomass Valor., 2 (2011) 87-94.
22. Ö. Ç. Sola, M. Yayla, B. Sayın, C.D. Atiş, Adv. Mater. Sci. Eng., (2011) 1-6.
23. C. Leiva, L. Sanchez de Alcázar, C. Arenas, M. Rodriguez-Galan, B. Alonso-Fariñas, A. Cornejo, Y. Luna, Fired bricks with replacing clay by combustion fly ash in high volume ratio, 4th International Congress on Green Process Engineering (GPE 2014), Seville, Spain, 2014.
24. Y. Luna, C.G. Arenas, A. Cornejo, C. Leiva, L.F. Vilches, C. Fernández-Pereira, Int. J. Energ. Environ. Eng., 5 (2014) 387-397.
25. G. Makaka, Comput. Water Energ. Environ. Eng., 3 (2014) 152-161.
26. A. S. Pawar, D. B. Garud, IJRET: Int. J. Res. Eng. Technol., 03(09) (2014). eISSN: 2319-1163, pISSN: 2321-7308
27. V. Karayannis, X. Spiliotis, A. Domopoulou, K. Ntampegliotis, G. Papapolymerou, Rom. J. Mater., 45(4) (2015) 358-363.
28. S. Abbas, M.A. Saleem, S.M.S Kazmi, M.J. Munir, J. Build. Eng., 14 (2017) 7-14.
29. D. Eliche-Quesada, J. A. Sandalio-Pérez, S. Martínez-Martínez, L. Pérez-Villarejo, P. J. Sánchez-Soto, Ceram. Int. 44 (2018) 4400-4412.

_____

30. M. Sutcu, E. Erdogmus, O. Gencel, A, Gholampour, E. Atan, T. Ozbakkaloglu, J. Clean. Prod., 233 (2019) 753-764.
31. P. G. Sonawane, A. K. Dwivedi, Am. J. Eng. Res. (AJER), 02(09) (2013) 110-117.
32. T. Gupta, K.A. Patel, S. Siggique, R.K. Sharma, S. Chaudhary, Measurement, 147 (2019) 106870. https://doi.org/10.1016/j.measurement.2019.106870
33. S. N. Mamdani, G. L. Rakesh, T. P. Mathew, Int. J. Sci. Eng. Technol. Res. (IJSETR), 4(5) (2015) 1478-1480.
34. M. Vasić, Z. Radojević, L. Pezo, Application of organic and inorganic wastes in clay brick production: A chemometric approach, In: Advanced ceramic materials, Ch. 8, pp. 300-335. Advanced materials series (edited by Ashutosh Tiwari, Rosario A. Gerhardt, and Magdalena Szutkowska), Scrivener publishing, Wiley, Beverly, USA, ISBN: 978-1-119-24244-4, 2016.
35. Zulkifli, G. Panji, Mater. Sci. Forum, 964 (2019) 270-279.
36. M. Arsenović, Z. Radojević, S. Stanković, . Ž. Lalić, L. Pezo, Ceram. Int. 39(2) (2013) 1667-1675.
37. L. Pezo, M. Arsenović, Z. Radojević, Ceram. Int., 40(7) (2014) 9637-9645.
38. G. Shafabakhsh, H. Naderpour, R. Noroozi, J. Rehabil. Civ. Eng., 3[1] (2015) 61-73.
39. Y. Yoon, G. Swales Jr, T. M. Margavio, J. Oper. Res. Soc., 44(1) (1993) 51-60.
40. U. Choudhury, Effect of fly ash addition on the properties of fired clay. BsC thesis, Department of ceramic engineering, National Institute of technology, Rourkela, 2015.
41. B. Yannick, W.A.S. Ludovic, N. Francois, K. K. Véronique, F. Nathalie, Sci. Sinter., 51 (2019) 57-70.
42. N. Tangboriboon, S. Moonsri, A. Netthip, W. Sangwan, A. Sirivat, Sci. Sinter., 51 (2019) 1-13.
43. M. V. Vasić, L. L. Pezo, J. D. Zdravković, M. Vrebalov, Z. Radojević, Sci. Sinter., 50 (2018) 487-500.
44. M. U. Rehman, M. Ahmad, K. Rashid, J. Build. Eng., 27 (2020) 100965.
45. A. Cheshomi, A. Eshaghi, J. Hassanpour, Appl Clay Sci., 135 (2017) 190-198.
46. L. Gredmaier, C. J. Banks, R. B. Pearce, Constr. Build. Mater., 25 (2011) 4477-4486.
47. J. C. Hower, Int. J. Coal Geol., 92 (2012) 90-97.
48. S. Petrović, V. Jovanov, S. Vujović, J. Ranogajec, E. Fidančevska, Process. Appl. Ceram., 1[1–2] (2007) 75-80.

Сажетак: *У овом истраживању анализирани су подаци о угљеним пепелима из термо-електрана који су се користили у производњи опеке у последњих 20 година. Статистичка анализа спроведена је на укупно 302 случаја на основу релевантних параметара из литературе. Као улазни подаци за моделовање изабрани су хемијски састав глина и угљених пепела, удео и максимална величина честица пепела, величина печених узорака, вршна температура печења и одговарајуће трајање синтеровања. Карактеристике производа као што су отворена порозност, упијање воде и чврстоћа на притисак узете су као излазни параметри. Развијен је модел у облику вештачке неуронске мреже, који је показао задовољавајуће поклапање са експерименталним подацима и који је предвидео посматране излазне параметре са коефицијентом детерминације (r^2) од 0,972, током периода учења мреже. Поред тога, редуковани хи-квадрат, средња грешка одступања, корен средње квадратне грешке и средња процентуална грешка коришћени су за проверу тачности предвиђања добијеног модела, чиме је доказана добра способност генерализације развијене мреже. Анализа осетљивости модела сугерисала је да су количине Na_2O из опекарских глина, затим удели SiO_2 и K_2O који потичу из пепела, као и садржај MgO у глинама опадајућим*

_____

редом најутицајнији на квалитет композитних опека од угљеног пепела и глине, што указује на важност присуства топитеља у процесу печења.

Кључне речи*: Опекарске глине, угљени пепео, традиционална керамика, механичка својства, математичко моделовање.*